Proceedings of the Institution of Mechanical Engineers, Part C: Journal of Mechanical Engineering Science
http://pic.sagepub.com/

Centre-Line Deviation as a Measure of Camber in Steel Slabs During Unrestricted Horizontal Rolling

R. J. Montague, J Watton and K. J. Brown

Proceedings of the Institution of Mechanical Engineers, Part C: Journal of Mechanical Engineering Science 2005 219: 775
DOI: 10.1243/095440605X31625

The online version of this article can be found at:
http://pic.sagepub.com/content/219/8/775

Published by:
SAGE
http://www.sagepublications.com

On behalf of:
Institution of Mechanical Engineers

Additional services and information for *Proceedings of the Institution of Mechanical Engineers, Part C: Journal of Mechanical Engineering Science* can be found at:

Email Alerts: http://pic.sagepub.com/cgi/alerts

Subscriptions: http://pic.sagepub.com/subscriptions

Reprints: http://www.sagepub.com/journalsReprints.nav

Permissions: http://www.sagepub.com/journalsPermissions.nav

Citations: http://pic.sagepub.com/content/219/8/775.refs.html

>> Version of Record - Aug 1, 2005

What is This?

Downloaded from pic.sagepub.com at Cardiff University on April 4, 2012

Centre-line deviation as a measure of camber in steel slabs during unrestricted horizontal rolling

R J Montague[1]*, **J Watton**[2], and **K J Brown**[3]
[1]Engineering Doctorate Centre, ECM[2], Port Talbot, UK
[2]School of Engineering, Cardiff University, Cardiff, UK
[3]Corus RD&T, Port Talbot, UK

The manuscript was received on 18 November 2004 and was accepted after revision for publication on 5 May 2005.

DOI: 10.1243/095440605X31625

Abstract: A theoretical analysis of slab motion during camber evolution in unrestricted horizontal rolling is presented. The analysis shows that a linear relationship exists between centre-line deviation (CLD) curvature and outgoing camber, which is a function of ingoing and outgoing slab thickness and ingoing slab camber.

An experimental study, undertaken during commercial rolling at the hot strip mill in Port Talbot, is described. CLD data from a stereoscopic width gauge (SWG) and a line scanning pyrometer (LSP) at the exit of the horizontal scale breaker were compared with the measurements of actual outgoing slab camber. The results confirmed the findings of the theoretical analysis and showed that CLD data, once suitably processed, can be used as a measure of camber. The SWG appeared to offer better measurements than the LSP. Incorporating ingoing camber into the model improved the accuracy achieved. Finally, a practical on-line camber measurement technique using SWG CLD data is proposed on the basis of the findings of this study.

Keywords: hot strip rolling, camber, modelling, centre-line deviation

1 INTRODUCTION

Camber is the longitudinal curvature of a slab or strip in the horizontal plane. It is induced during rolling when differences in conditions across the width of the material cause one edge to become longer than the other. Camber leads to process instability, which can cause operational difficulties and/or adversely affect product quality.

Although camber has been recognized as a problem for many years, progress in this area has been held back by the difficulty in obtaining quantitative on-line measurements of the phenomenon. For this reason, the majority of studies published have been based on qualitative assessment, pilot plant trials, or simulation [**1**–**5**].

Attempts have been made to measure camber by recording the centre-line deviation (CLD) of a slab or strip as it passes a fixed point. Such measurements have been reported to be successful as a qualitative feedback tool for operators [**4**]. However, doubt has been cast on the ability of this method to distinguish between rotation and lateral slipping (tracking) and actual curvature [**5**, **6**]. Systems that make multiple CLD measurements simultaneously have been developed to overcome this problem [**6**–**8**], but the cost of these is correspondingly higher.

In the present study, an analytical study of slab behaviour at the horizontal scale breaker (HSB) in the hot strip mill at Port Talbot was undertaken. It was shown that it should be possible to use single-point CLD measurements to calculate the camber of slabs as they are rolled. This conclusion was validated using the data collected during commercial rolling operations. On the basis of these results, a practical solution for on-line measurement of camber using CLD data is presented.

The systems used to make CLD measurements were a CCD2001 stereoscopic width gauge (SWG) manufactured by Shape Technology Ltd [**9**] (formerly European Electronic Systems) and a LANDSCAN LS11 line scanning pyrometer (LSP) manufactured by LAND Instruments International [**10**]. The positions of these devices at the exit of the HSB are shown in Fig. 1.

Corresponding author: 85 Allport Road, Cannock, Staffordshire WS11 1DY, UK. email: montaguerj@hotmail.com

Downloaded from pic.sagepub.com at Cardiff University on April 4, 2012

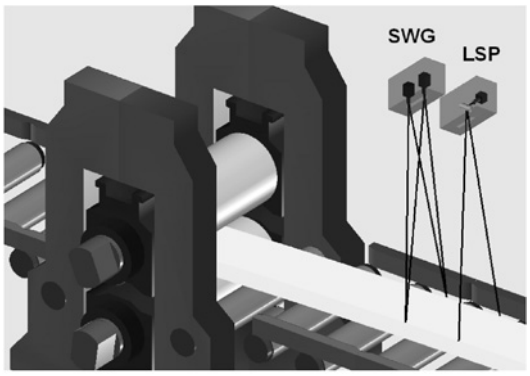

Fig. 1 SWG and LSP shown measuring a slab at the exit of the HSB in the Port Talbot hot strip mill

2 ANALYSIS

In the analytical modelling of camber, a linear difference in reduction across a slab's width has generally been assumed. Under conditions of no lateral spread (plane strain), any variation in reduction causes a corresponding difference in elongation and velocity. This leads to the development of a curvature at the roll gap exit and rotation of the head and tail ends of the slab.

The ingoing and outgoing velocities of the slab can be found from basic rolling theory (Fig. 2(a)). At the neutral point (ϕ_N), the velocity of the slab (v_N) is equal to the peripheral speed of the rolls ($R\omega_{roll}$). The thickness at this point (h_N) can be found by solution of Sims' rolling equations [**11**]. The ingoing and outgoing velocities (v_{in} and v_{out}, respectively) can therefore be found from the ingoing and outgoing thickness values (H and h, respectively) by assuming volume constancy through the roll bite. A concept often used in rolling is forward slip (s_f), which relates v_{out} to v_N: $v_{out} = (1 + s_f)v_N$. The value of s_f is therefore $h_N/h - 1$.

Hayashi and Kono [**12**] modelled the evolution of camber on the basis of the analysis of the movements illustrated in Fig. 2(b). The ingoing (tail) and outgoing (head) rotations (ω_{in} and ω_{out}, respectively) were found from the difference between ingoing and outgoing velocities at the strip edges. To do this, they calculated the forward slip independently for the drive and operator sides of the strip, assuming that $S_f = r/4$, where reduction, $r = 1 - h/H$. This assumption is not valid for all rolling geometries. A generalized form of this relationship ($s_f = r/n$) was therefore derived from Sims' equations, which can be shown to hold for any given geometry

$$n = \left(1 - \frac{h}{H}\right)\cot^2\left(\frac{\pi}{8}\sqrt{\frac{h}{R}}\ln\frac{h}{H} + \frac{1}{2}\tan^{-1}\sqrt{\frac{H-h}{h}}\right) \quad (1)$$

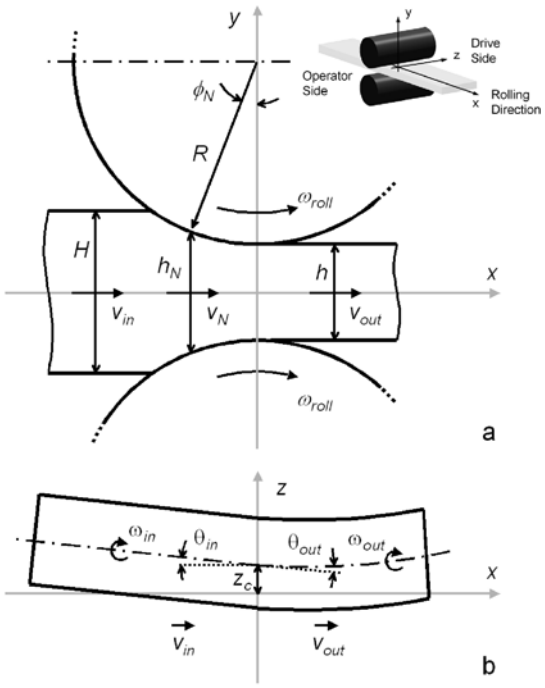

Fig. 2 (a) Vertical section through rolls and slab showing constant volume flow during plane strain rolling and (b) plan view of slab showing rigid body motion during camber evolution

Using this relationship, slab rotation could be found in terms of a linear difference in reduction (elongation). This difference was represented in terms of a specific wedge factor ($\Delta\Psi$)

$$\Delta\Psi = \frac{H_{op} - H_{dr}}{WH} - \frac{h_{op} - h_{dr}}{Wh} \quad (2)$$

where subscript op refers to the thickness on the operator side of the slab, subscript dr refers to the value on the drive side of the slab, and no subscript refers to an average value across the slab's width (W).

The slab motions in Fig. 2(b) can now be defined in terms of the work roll speed, specific wedge factor, n, and the slab elongation, $\lambda = H/h$. Their definitions are given by

$$v_{in} = v_N\frac{1}{n\lambda}\left(n + 1 - \frac{1}{\lambda}\right) \quad (3a)$$

$$v_{out} = v_N\frac{1}{n}\left(n + 1 - \frac{1}{\lambda}\right) \quad (3b)$$

$$\omega_{in} = v_N\frac{\Delta\Psi}{n\lambda}\left(n + 1 - \frac{2}{\lambda}\right) \quad (3c)$$

$$\omega_{out} = -v_N\frac{\Delta\Psi}{n\lambda} \quad (3d)$$

Downloaded from pic.sagepub.com at Cardiff University on April 4, 2012

Nakajima *et al.* [**13**] evaluated the snaking of strip by making the assumption that the material could be considered to move as a rigid body. In this way, the evolution of the slab centre-line at the entry to the roll gap (x_{in}, z_{in}) with time (t) was modelled as

$$x_{in}(t) = \int v_{in}(t) + z_{in}(t)\omega_{in}(t)\mathrm{d}t \tag{4a}$$

$$z_{in}(t) = -\int x_{in}(t)\omega_{in}(t)\mathrm{d}t \tag{4b}$$

In the present application, v_{in} was constant and z_{in} was assumed to remain relatively small. This allowed equation (4) to be rewritten as

$$x_{in}(t) = x_0 + v_{in}t \tag{5a}$$

$$z_{in}(t) = -\int (x_0 + v_{in}t)\omega_{in}(t)\mathrm{d}t \tag{5b}$$

where x_0 was the slab's position along the x-axis at $t = 0$.

Most analyses of camber have assumed that $\Delta\Psi$ is a function of the slab or strip off-centre at the roll bite (z_c). This is because rolling a slab or strip away from the centre-line of the mill results in an asymmetrical force distribution, causing one side of the mill to stretch more than the other. This changes $\Delta\Psi$ and so ω_{in} varies throughout the deformation, complicating the analysis. However, off-centre rolling at the HSB has been shown to have a limited direct influence on camber [**1**]. This is because the HSB is a two-high rolling stand and so roll bending is substantial. This imparts a large crown to the slab, which compensates for differential mill stretching, as described by Nakajima *et al.* [**13**] and Stukach [**14**]. It can therefore be assumed that $\Delta\Psi$ and ω_{in} remain constant throughout the deformation. This makes it possible to arrive at a closed-form solution of equation (5b)

$$z_{in}(t) = z_0 - x_0\omega_{in}t - \frac{1}{2}v_{in}\omega_{in}t^2 \tag{6}$$

Measurements have shown that, before they were rolled, slabs had constant curvatures along their lengths (κ_{in}). The ingoing form of a slab of length L and initial off-centre at the roll gap z_{c_0} was therefore given by $f_0(x) = (1/2)\kappa_{in}x^2 + (1/2)\kappa_{in}Lx + z_{c_0}$. The slab's position along the z-axis at time $t = 0$ (z_0) was found from $f_0(x_0)$, inclined at an angle θ_0. The evolution of the slab's centre-line on the entry side of the mill (for $x \le 0$) was therefore

$$z_{in}(t) = f_0(x_0) - (\theta_0 + \omega_{in}t)x_0 - \frac{1}{2}v_{in}\omega_{in}t^2 \tag{7}$$

As the head end of a slab emerges from the rolls, its position along the x-axis (x_{out}) lies between $x = 0$ and $x = v_{out}t$. The z-position on the exit side of the roll gap (z_{out}) was determined by the outgoing angle (θ_{out}), the off-centre at the roll gap (z_c), and the outgoing curvature (κ_{out}), as given by

$$z_{out}(t) = \frac{1}{2}\kappa_{out}x_{out}(t)^2 - \theta_{out}(t)x_{out}(t) + z_c(t) \tag{8}$$

The outgoing angle was equal to the integral of ω_{out} added to the ingoing angle (θ_{in}), modified by stretching in the x-direction, to give $\theta_{out} = \theta_{in}/\lambda + \omega_{out}t$. The ingoing angle was given by $\theta_0 + \omega_{in}t$. The off-centre at the roll gap was found by making the substitution $x_0 = x_{in} - v_{in}t$ in equation (7) and solving for $x_{in} = 0$. This gave $z_c(t) = f_0(-v_{in}t) + \theta_0 v_{in}t + \frac{1}{2}v_{in}\omega_{in}t^2$. The outgoing centre-line profile was therefore

$$z_{out}(t) = \frac{1}{2}\kappa_{out}x_{out}^2 - \left(\frac{\theta_0 + \omega_{in}t}{\lambda} + \omega_{out}t\right)x_{out} + f_0(-v_{in}t) + \theta_0 v_{in}t + \frac{1}{2}v_{in}\omega_{in}t^2 \tag{9}$$

Equation (9) gives the time-varying CLD at any point along the x-axis. For a measurement device located d metres downstream of the roll axis, the time-varying CLD trace $z_{CLD}(t)$ was found by making the substitution $x_{out} = d$. This resulted in a quadratic in time. The time axis could then be converted to a distance (along the length of the slab) using the known constant exit velocity by making the substitution $t = x/v_{out}$. The curvature (κ_{CLD}) of the resulting distance-based CLD trace $z_{CLD}(x)$ was then given by

$$\kappa_{CLD} = \frac{\mathrm{d}^2 z_{CLD}(x)}{\mathrm{d}x^2} = \frac{1}{\lambda}\frac{\omega_{in}}{v_{out}} + \frac{1}{\lambda^2}\kappa_{in} \tag{10}$$

Note that the position of the measurement device along the x-axis (d) does not appear in equation (10). When the relevant definitions of equation (3) were substituted into equation (10), the following relationship was found

$$\kappa_{CLD} = \frac{\Delta\Psi}{\lambda^2}\left(\frac{n\lambda + \lambda - 2}{n\lambda + \lambda - 1}\right) + \frac{1}{\lambda^2}\kappa_{in} \tag{11}$$

The concept of a curvature ratio (CR) was then introduced to help describe the behaviour of the slab. Curvature ratio was defined as

$$\mathrm{CR} = \frac{\Delta\kappa}{\kappa_{CLD} - (1/\lambda^2)\kappa_{in}} \tag{12}$$

Downloaded from pic.sagepub.com at Cardiff University on April 4, 2012

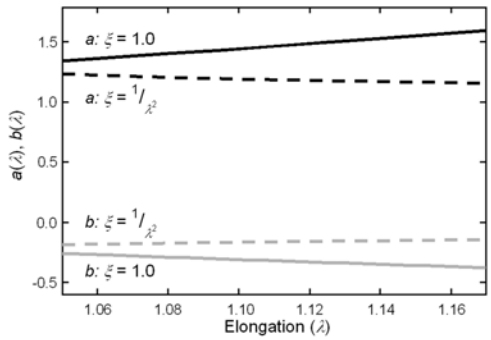

Fig. 3 Parameters a and b shown as a function of elongation and camber coefficient

where $\Delta\kappa$ is the change in curvature induced by rolling. The relationship between $\Delta\kappa$ and κ_{out} has been commonly stated as $\kappa_{\text{out}} = \kappa_{\text{in}}/\lambda^2 + \Delta\kappa$. The calculation of $\Delta\kappa$ has been suggested to take the form $\Delta\kappa = \xi\Delta\Psi$, where ξ is the camber change coefficient. Previous authors have ascribed values of either $1/\lambda^2$ or unity to this variable under most rolling conditions [**2**, **7**, **8**, **12**, **13**]. Substituting these definitions into equations (11) and (12) gives

$$\kappa_{\text{out}} = \kappa_{\text{CLD}}\text{CR} + \kappa_{\text{in}}\frac{1}{\lambda^2}\left(\frac{1-\text{CR}}{\text{CR}}\right) \tag{13a}$$

$$\kappa_{\text{out}} = a\kappa_{\text{CLD}} + b\kappa_{\text{in}} \tag{13b}$$

$$\text{CR} = \xi\lambda^2\left(\frac{n\lambda+\lambda-1}{n\lambda+\lambda-2}\right) \tag{14}$$

Figure 3 shows functions a and b in equation (13b) evaluated over the typical range of conditions at the HSB ($H = 0.234$ m; $1.05 \leq \lambda \leq 1.17$) for the two most commonly stated values of ξ. Although work roll radius appears as a factor in n, its effect on these functions is negligible within the range of values found at the HSB ($0.432 \leq R \leq 0.457$ m).

3 EXPERIMENTAL RESULTS

3.1 Data collection

To validate the preceding theoretical analysis, trials were performed at the Port Talbot hot strip mill. The aim of these trials was to determine whether CLD measurements could be used as a practical measure of camber. To do this, a measure of the actual curvature of the slabs as they left the HSB (κ_{out}) was required.

The method used required the application of an image processing camber measurement technique developed by the authors [**15**]. In brief, this involved capturing an image of the slab on the roller tables at the exit of the HSB (Fig. 4(a)). This picture was transformed to a planar view and the centre-line of the slab was extracted, from which its curvature could be calculated (Fig. 4(b)). The curvature measurements made in this way were compared with the CLD data collected using SWG and LSP systems.

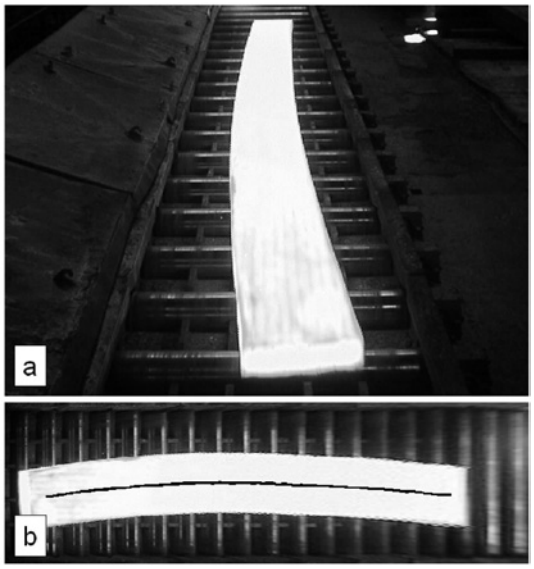

Fig. 4 (a) Photograph of a cambered slab on the transfer tables at the exit of the HSB at Port Talbot and (b) plan view of the same scene showing the extracted slab centre-line

The models established in this paper are valid only for CLD data recorded, while a slab remains engaged in the HSB roll gap. During this time, its dynamics are dominated by rolling forces and so its motion is predictable. However, once a slab is free of the roll stand, its position may be subject to unpredictable rotation and lateral movements and its speed does not remain constant. The latter parts of the CLD traces were therefore unsuitable for curvature measurement and so had to be trimmed.

For the LSP, the CLD traces were trimmed in the following way. The scheduled slab length was multiplied by the elongation to give its length as it exited the HSB. The distance (d) from the roll gap exit to the LSP was known and so the length of slab over which valid CLD data were generated could be found. From the knowledge of the slab's speed and the sampling rate of the LSP, the number of valid line scans could be deduced and used to trim the CLD data. The time axis was then converted to a distance using the outgoing velocity and a least squares quadratic fit was found, as shown in Fig. 5. The average curvature of the LSP CLD data (κ_{LSP}) was extracted from the equation of this line as twice the x^2 coefficient.

The computer that recorded the CLD data from the SWG also logged the HSB motor current. This current

Downloaded from pic.sagepub.com at Cardiff University on April 4, 2012

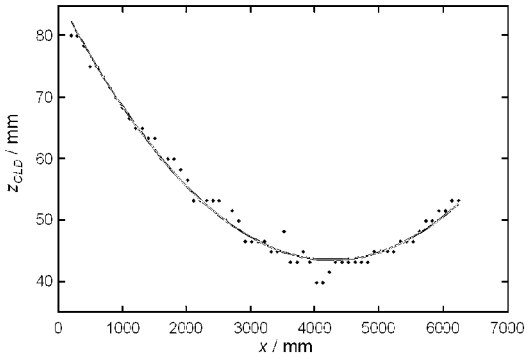

Fig. 5 Trimmed LSP CLD data plotted against slab length showing a least squares quadratic fit

increased significantly when a slab was in the roll bite, which made it easy to trim the CLD trace to include only the applicable data, as illustrated in Fig. 6. The time axis in Fig. 6 was converted to a distance and the average curvature of the SWG CLD data (κ_{SWG}) was found in the same way as for the LSP measurements.

3.2 Results analysis

Figure 7 shows the results of these trials, comprising 165 slabs measured by the SWG and 185 slabs measured by the LSP. Least squares linear fits were calculated for both data sets and plotted on the graphs in Fig. 7. The CLD curvatures showed good correlation with the image-processed measurements. The fit to the LSP data had an R^2 value of 0.85. This rose to 0.92 for the SWG measurements, reflecting their somewhat tighter grouping.

An estimate of the outgoing curvatures could therefore be made by simply dividing the measured CLD curvatures by the gradients of the least squares fits. This could be considered equivalent to using an average curvature ratio ($\overline{CR}$) as a in equation (13b) and by setting b to zero.

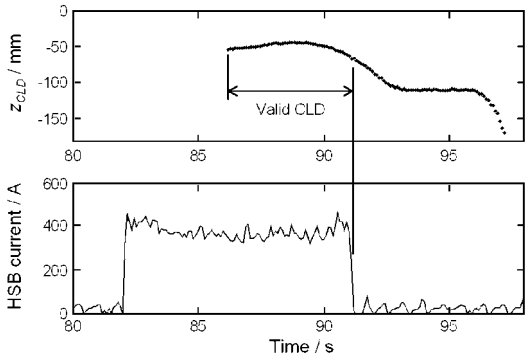

Fig. 6 Motor current and SWG CLD recorded as a slab passes through the HSB

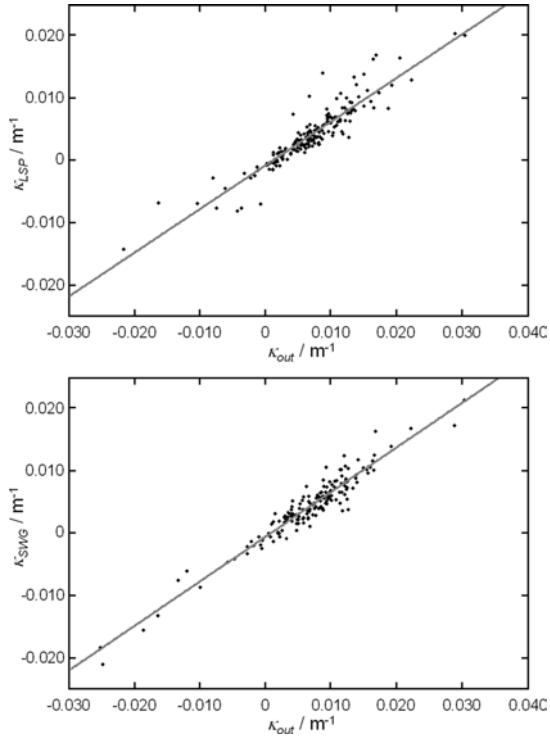

Fig. 7 SWG and LSP CLD curvatures plotted against image-processed slab curvature measurements

The gradients of the linear trends were 0.72 for the SWG data and 0.70 for the LSP data, equating to $\overline{CR}$ values of 1.38 and 1.43, respectively. The average of the CR values calculated using equation (14) for each of the slabs in the trials was 1.45 for the SWG data and 1.47 for the LSP data, using a camber change coefficient of 1.0. Using a camber change coefficient of $1/\lambda^2$, the average values of CR were 1.19 for both the SWG and the LSP data. This suggested that the camber change coefficient was probably close to unity.

Estimates of slabs' outgoing curvatures were found by applying this version of equation (13b) to the CLD data sets, using the gradients of the linear trends as the average curvature ratio. The errors between these estimates and the observed curvatures (κ_{out}) were then calculated. The main features of the error distributions are given in Table 1.

If the uncertainty of measurement (at the 95 per cent confidence level) can be approximated by twice

Table 1 Summary of SWG and LSP CLD curvature error distributions found using equation (13b) with $a = \overline{CR}$ and $b = 0$

Measurement system	Average curvature error (m^{-1})	Estimate of the standard deviation (m^{-1})
SWG	-0.7×10^{-3}	2.1×10^{-3}
LSP	-0.7×10^{-3}	2.6×10^{-3}

Downloaded from pic.sagepub.com at Cardiff University on April 4, 2012

the estimate of the standard deviation plus the magnitude of the average error, the accuracy achieved using the SWG was $4.9 \times 10^{-3}\,\mathrm{m}^{-1}$. For the LSP system, this value was $5.9 \times 10^{-3}\,\mathrm{m}^{-1}$.

The superior accuracy of the SWG was probably due to three major factors. The first was that the resolution of the CLD data offered by the SWG was finer than that of the LSP system by almost an order of magnitude. The second was that the SWG cameras were located upstream of the LSP scanning head (as shown in Fig. 1). This meant that more of each slab was measured while it was in the roll gap and so a greater number of CLD data points were available with which the curvature was calculated. Finally, the way in which the CLD traces were trimmed was more reliable for the SWG data than for the LSP measurements. The direct use of the HSB motor current left little scope for error with the SWG, but the approach that had to be adopted for the LSP data relied on an assumption that both the scheduled slab length and the calculated elongation were correct.

The information in Table 1 quantifies the ability of the single variable, κ_{CLD}, to measure the camber of slabs at the exit of the HSB. However, the theoretical analysis suggested that the relationship between κ_{CLD} and κ_{out} also depended on the curvature of the slabs prior to being rolled in the HSB (κ_{in}). A laser-based slab geometry measurement system (SGMS) has recently been commissioned at the entry to the reheat furnaces of the hot mill in Port Talbot. This measures the width, camber, and thickness profiles of slabs as delivered to the mill. Data from this system were used to find κ_{in}.

Ingoing slab camber information was available for all of the slabs measured by the LSP. However, some of the SWG data were collected before the SGMS had been fully commissioned. Because of this, 100 of the slabs for which SWG data were collected had no corresponding SGMS camber measurements. The measurements from the remaining 65 slabs were processed in the same way as described earlier.

The gradient of the least squares linear fit was 0.70, corresponding to a value of 1.44 for $\overline{\mathrm{CR}}$. The values calculated from theory were $\overline{\mathrm{CR}} = 1.44$ using a camber change coefficient of 1.0 and $\overline{\mathrm{CR}} = 1.20$ using Nakajima's value of $1/\lambda^2$. The mean error was $-0.8 \times 10^{-3}\,\mathrm{m}^{-1}$ and the estimate of the standard deviation of the error distribution was $2.6 \times 10^{-3}\,\mathrm{m}^{-1}$, giving an estimate of accuracy of $6.0 \times 10^{-3}\,\mathrm{m}^{-1}$ at the 95 per cent level of certainty.

Multiple linear regression was then used to relate CLD curvature and ingoing camber to actual outgoing curvature on the basis of equation (13b). As shown in Fig. 3, under the range of conditions experienced at the HSB, the functions a and b were predicted to be relatively linear with respect to λ (the maximum error introduced by this simplification was predicted to be <4 per cent). A model was therefore formed with $a = a_0 + a_1\lambda$ and $b = b_0 + b_1\lambda$. This was readily solved to find the unknown constants for both the SWG and LSP datasets. The resulting functions a and b are shown in Fig. 8, evaluated over the range of conditions experienced during these trials and overlaid on the predicted values shown in Fig. 3.

The results in Table 2 show that the measurement of camber using CLD data becomes more accurate if the ingoing camber is also considered. This improvement also suggests that the linear equations in λ used to approximate the functions a and b were effective.

The comparison of these derived functions with those predicted by theory (Fig. 8) suggests that the theoretical model developed was a reasonable approximation to reality. The magnitude and trend of function a found by the regression study was consistent between SWG and LSP data sets and similar to the values of CR predicted by equation (14). The prediction of function b was less successful; the regression study suggested that ingoing camber exerts a larger influence than that was suggested by theory. However, the experimental results do

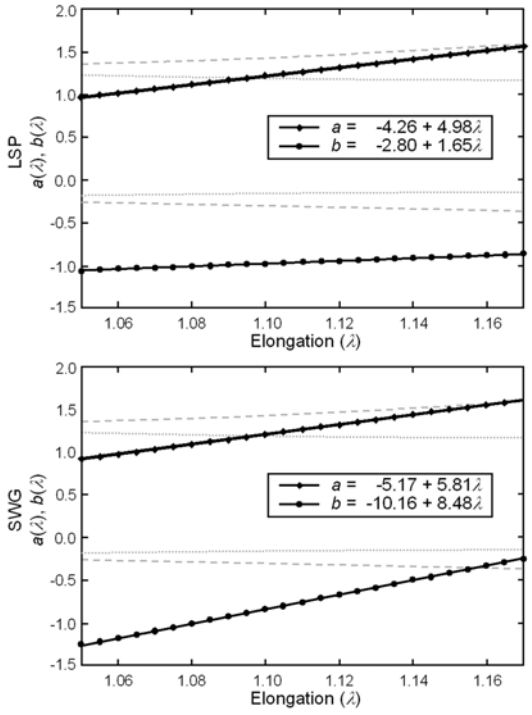

Fig. 8 Functions $a(\lambda)$ and $b(\lambda)$ found by multiple linear regression using SWG and LSP data. Dashed lines show the theoretical values expected for functions a and b with $\xi = 1.0$. Dotted lines show the theoretical values of these functions with $\xi = 1/\lambda^2$

Downloaded from pic.sagepub.com at Cardiff University on April 4, 2012

Table 2 Summary of SWG and LSP CLD curvature error distributions found using equation (13b) with a and b found by multiple linear regression

Measurement system	Average curvature error (m^{-1})	Estimate of the standard deviation (m^{-1})
SWG	-0.2×10^{-3}	2.2×10^{-3}
LSP	-0.7×10^{-3}	2.3×10^{-3}

confirm that the effect of ingoing camber is negative. There was also an apparent difference in the behaviour of function b between SWG and LSP datasets. This may have been because all of the slabs on which the SWG study was performed exhibited negative ingoing cambers. The regression would therefore have used this fact to reduce the average curvature error, distorting the true effect of the variable.

The final model proposed to relate the CLD measurements and ingoing camber to the outgoing camber was

$$\kappa_{\text{out}} = (a_0 + a_1\lambda)\kappa_{\text{CLD}} + (b_0 + b_1\lambda)\kappa_{\text{in}} + c \qquad (15)$$

The model in equation (15) differed from equation (13b) only by a constant term (c). The theoretical analysis did not point to the existence of such a parameter, but the non-zero average curvature errors in Tables 1 and 2 suggested that its inclusion would be of benefit. Again, regression was used to find the unknown parameters for both datasets. The results in Table 3 show that equation (15) provided superior predictions of the outgoing camber to the foregoing models. The average error was reduced to zero and the spread of the predictions became narrower using the more complex equation.

The best accuracy achieved by the LSP was $4.4 \times 10^{-3}\,m^{-1}$ using equation (15). This was an improvement of $1.6 \times 10^{-3}\,m^{-1}$ over the accuracy achieved using equation (13b) with $a = \overline{CR}$ and $b = 0$. For the slabs measured by both the SWG and the SGMS, the best accuracy was $4.2 \times 10^{-3}\,m^{-1}$, an improvement of $1.8 \times 10^{-3}\,m^{-1}$ over the simplest model. On the basis of a comparison of the results in Table 1, it is possible that a superior figure for SWG accuracy could be attained, given a larger and more representative sample of slabs to work with. If a similar improvement were to be seen with the more advanced model, the best accuracy expected would be $3.1 \times 10^{-3}\,m^{-1}$. However, this could only be achieved at the expense of a requirement for more information, especially in the form of ingoing camber measurements, which were not always available.

Table 3 Summary of SWG and LSP CLD curvature error distributions found using equation (15) with a, b, and c found by multiple linear regression

Measurement system	Average curvature error (m^{-1})	Estimate of the standard deviation (m^{-1})
SWG	0.0×10^{-3}	2.1×10^{-3}
LSP	0.0×10^{-3}	2.2×10^{-3}

3.3 Practical camber measurement

The aim of this work was to provide a practical measure of camber at the exit of the HSB. The slabs measured in this study were shown to exhibit curvatures in excess of $25 \times 10^{-3}\,m^{-1}$ at this point. Therefore, even the simplest method of CLD analysis had the ability to determine camber effectively on a simple scale of ± 5 points. A camber of '-5' would be reported if a slab were severely cambered to the operator side (i.e. $\kappa_{\text{out}} = -25 \times 10^{-3}\,m^{-1}$). If the slab were straight (i.e. $\kappa_{\text{out}} = 0\,m^{-1}$), the system would report '0' and it would report '+5' if the slab were severely cambered to the drive side (i.e. $\kappa_{\text{out}} = -25 \times 10^{-3}\,m^{-1}$).

The processing requirements to do this are modest and require just SWG data and HSB motor current; a flow chart summarizing the steps involved is shown in Fig. 9. This user-friendly measurement would be

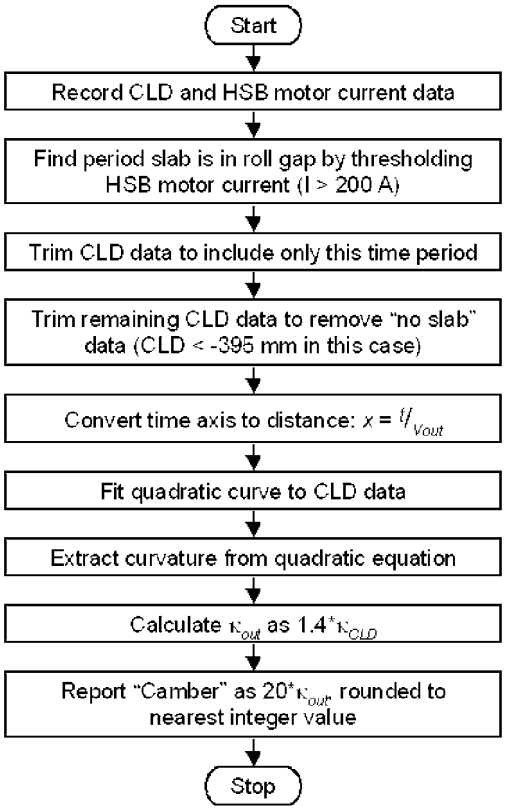

Fig. 9 Flow diagram showing each step required to measure curvature using CLD data

Downloaded from pic.sagepub.com at Cardiff University on April 4, 2012

sufficient to allow the operator to make informed decisions (for example, whether to adjust the reversing rougher entry guides) and would help with HSB roll levelling. If this data were archived, it could also be used as a historical performance indicator. If finer resolutions were required, SGMS curvature measurements could be incorporated into a more complete model, such as equation (15). This would deliver an improvement in resolution to approximately ± 7 points.

The analysis of camber measurement using CLD data presented in this work is restricted to the conditions found at the HSB in Port Talbot. In most roughing stands, the assumption of unrestricted horizontal rolling will not be valid because of edging and guiding practices. The analysis certainly does not extend to tandem mills such as the finishing train, where large interactions exist between stands. Finally, the assumption that off-centre has no effect on camber is valid only where strip crowns are large in relation to differential mill stretching. Therefore, although CLD data may be suitable for camber measurement elsewhere in the roughing mill, further investigation would be required to confirm this.

4 CONCLUSIONS

CLD measurements have been shown to be suitable for camber measurement in unrestricted horizontal rolling. A theoretical analysis of slab behaviour proposed a linear relationship that was a function of ingoing and outgoing slab thickness and ingoing slab camber. This relationship was confirmed by experimental data obtained during commercial rolling at the hot strip mill in Port Talbot.

Using the relationship $\kappa_{\text{out}} = \kappa_{\text{CLD}}\overline{\text{CR}}$, it was shown that the SWG could measure outgoing curvature with an accuracy of $4.9 \times 10^{-3}\,\text{m}^{-1}$ at the 95 per cent confidence level. It was then demonstrated that this accuracy could be improved by up to $1.8 \times 10^{-3}\,\text{m}^{-1}$ if ingoing camber and elongation were incorporated into the analysis, using the relationship $\kappa_{\text{out}} = (a_0 + a_1\lambda)\kappa_{\text{CLD}} + (b_0 + b_1\lambda)\kappa_{\text{in}} + c$.

On the basis of these findings, a practical, on-line camber measurement technique was proposed. The simplest measurement model was selected because it required no additional data from other sources, making the system robust to a wider range of operating conditions. The camber of each bar would be represented as an integer value, from -5 (severely cambered to the operator side), through 0 (straight), to $+5$ (severely cambered to the drive side). This information could be used to improve roughing operations and as an indicator of mill camber performance.

REFERENCES

1 **Biggs, D. L., Hardy, S.,** and **Brown, K. J.** Influence of process variables on development of camber during hot rolling of strip steel. *Ironmaking Steelmaking*, 2000, **27**(1), 55–62.

2 **Shiraishi, T., Ibata, H., Mizuta, A., Nomura, S., Yoneda, E.,** and **Hirata, K.** Relation between camber and wedge in flat rolling under restrictions of lateral movement. *ISIJ Int.*, 1991, **31**(6), 583–587.

3 **Nilsson, A.** FE simulations of camber in hot strip rolling. *J. Mater. Process. Technol.*, 1998, **80–81**, 325–329.

4 **Loney, D. W.** *Optimisation of the use of strip geometry control system (EUR 20101 EN)*, 2002 (RFCS Publications, Luxembourg).

5 **Tucker, B. J. S.** *Understanding camber for improved straightness of hot rolled coil.* MRes Thesis, University of Wales, Swansea, 2000.

6 **Piot, J. P., Tonnon, E.,** and **Dowdey, B.** *Hot strip roughing mill: camber measurement (EUR 20644 EN)*, 2003 (RFCS Publications, Luxembourg).

7 **Tanaka, Y., Omori, K., Miyake, T., Nishizaki, K., Inoue, M.,** and **Tezuka, S.** Camber control techniques in plate rolling. *Kawasaki Steel Tech. Rep.*, 1987, **16**, 12–20.

8 **Wakatsuki, K., Dairiki, O.,** and **Mabuchi, H.** Development of plate rolling technology at NSC Oita Works. In ATS-IRSID 4th International Steel Rolling Conference, Deauville, 1–3 June 1987, Conference Proceedings Vol. 2, C3.1–C3.11.

9 **Shape Technology Ltd,** 11 Enterprise Way, Aviation Park West, Christchurch, Dorset, BH23 6EW, UK.

10 **LAND Instruments International,** Dronfield, S18 1DJ, UK.

11 **Sims, R. B.** The calculation of roll force and torque in hot rolling mills. *Proc. Instn Mech. Engrs*, 1954, **168**, 191–200.

12 **Hayashi, C.** and **Kono, T.** Analysis of the camber generating mechanism in a strip mill. *Tetsu-to-Hagané*, 1977, **63**(2), A21–A24 (in Japanese).

13 **Nakajima, H., Kikuma, S., Matsumoto, H., Kajiwara, T., Kimura, T.,** and **Takawa, M.** Research into methods for controlling snaking in hot strip rolling. In 1980 Japanese Spring Conference for the Technology of Plasticity, Kitakyushu, 21–23 May 1980, Conference Proceedings, Article 116, 61–64 (in Japanese).

14 **Stukach, A. G.** Rolling of sheet and strip in rolls positioned at an angle to each other. *Tsventn. Met.*, 1978, **3**, 58–60 (in Russian).

15 **Montague, R. J., Watton, J.,** and **Brown, K. J.** A machine vision measurement of slab camber in hot strip rolling. *J. Mater. Process. Technol.*, in press.

APPENDIX

Notation

a	influence of κ_{CLD} on κ_{out}
b	influence of κ_{in} on κ_{out}
c	constant influence on κ_{out}
CR	curvature ratio
$\overline{\text{CR}}$	average curvature ratio

Downloaded from pic.sagepub.com at Cardiff University on April 4, 2012

d	distance along x-axis from rolls
f_0	shape of slab before rolling
h	outgoing thickness
h_N	thickness at neutral point
H	ingoing thickness
L	slab length
n	forward slip multiplier $= r/s_f$
r	reduction
R	work roll radius
s_f	forward slip
t	time
v_{in}	ingoing slab velocity
v_N	peripheral work roll velocity
v_{out}	outgoing slab velocity
W	slab width
x_{in}	position of slab tail on x-axis
x_{out}	position of slab head on x-axis
x_0	position of slab tail on x-axis at $t = 0$
z_c	slab off-centre at roll gap
z_{c_0}	slab off-centre at roll gap at $t = 0$
z_{CLD}	CLD trace
z_{in}	position of slab tail on z-axis
z_{out}	position of slab head on z-axis
z_0	position of slab tail on z-axis at $t = 0$
ϕ_N	angular location of neutral point
κ_{in}	ingoing slab curvature
κ_{out}	outgoing slab curvature
κ_{CLD}	curvature of CLD trace
κ_{LSP}	LSP CLD curvature
κ_{SWG}	SWG CLD curvature
λ	elongation
θ_{in}	angle of tail to rolling direction
θ_{out}	angle of head to rolling direction
θ_0	angle of tail to rolling direction at $t = 0$
ω_{in}	angular velocity of slab tail
ω_{out}	angular velocity of slab head
ω_{roll}	work roll angular velocity
ξ	camber change coefficient
$\Delta\kappa$	change in curvature
$\Delta\Psi$	specific wedge factor

Subscripts

dr	refers to a value on the drive side of the slab
op	refers to a value on the operator side of the slab

Downloaded from pic.sagepub.com at Cardiff University on April 4, 2012